

Velocity/Pressure-Gradient Correlations in a FORANS Approach to Turbulence Modeling

Svetlana V. Poroseva¹

University of New Mexico, Albuquerque, New Mexico, 87131

Scott M. Murman²

NASA Ames Research Center, CA 94035

The accuracy and reliability of turbulence models based on the Reynolds-Averaged Navier-Stokes equations depend on accuracy of modeling turbulent diffusion, interaction of turbulent pressure and velocity fields, and dissipative processes. In fourth-order statistical closures (FORANS models), the turbulent diffusion needs to be modeled only in transport equations of the fourth-order velocity moments. When the Gram-Charlier series expansion is used, such modeling can be achieved without unknown model coefficients and assuming the Gaussian turbulence. In the current paper, a consistent approach to modeling the velocity – pressure-gradient correlations of second, third-, and fourth-order velocity correlations with a limited number of model coefficients is discussed. New models for “slow” and “rapid” terms of the velocity – pressure-gradient correlations of different orders are proposed. The model expressions are verified using available DNS data in a two-dimensional channel flow and a zero-pressure gradient boundary layer over a flat plate.

Nomenclature

u_τ	=	friction velocity
U_i	=	mean velocity component in the i -direction
U	=	mean velocity in the streamwise direction in two-dimensional planar flows
$\Pi_{ij}, \Pi_{ijk},$	=	velocity – pressure-gradient tensors of second-, third-, and fourth ranks in FORANS equations
Π_{ijkl}		
u_i	=	velocity fluctuation in the i -direction
u, v, w	=	velocity fluctuations in streamwise, normal-to-wall, and spanwise directions in two-dimensional planar flows
x, y, z	=	streamwise, normal-to-wall, and spanwise directions in two-dimensional planar flows
δ_{ij}	=	Kronecker delta tensor
ν	=	kinematic viscosity
p	=	pressure fluctuation
r	=	distance between two points in a flow
y_+	=	yu_τ / ν
$f_{i,j}$	=	$\partial f_i / \partial x_j$
$\partial / \partial n$	=	normal derivative
$\langle \dots \rangle$	=	ensemble averaging

I. Introduction

When it comes to the accuracy of turbulence representation, the approach based on solving Reynolds-Averaged Navier-Stokes (RANS) equations has an unlimited potential. Indeed, the solution of the complete set of exact

¹ Assistant Professor, Mechanical Engineering, MSC01 1105, 1 UNM Albuquerque, NM 87131-0001, AIAA Associate Fellow.

² Aerospace Engineer, NASA Ames Research Center, Moffett Field, CA 94035.

RANS equations, velocity moments of different orders $\langle u_i^n u_j^m u_k^l \rangle$, where $n + m + l \geq 2$, and n, m , and $l = 0, 1, \dots, \infty$, completely describe a turbulent flow structure¹. In the general case, finding the accurate solution of the complete set of RANS equations is impossible, because it requires solving an infinite number of equations. However, for practical purposes, only some flow characteristics and their accurate representation are of importance. Thus, only velocity moments linked to the flow characteristics of interest should be reproduced accurately. This has been a motivation for developing the “closure” procedure and statistical closures of various orders. The first works in this direction can be traced back to Refs. 2-4.

The entire family of RANS closures can be viewed as a hierarchy. The higher the closure order, the more accurate the approximation is to the solution of the complete set of RANS equations. One- and two-equation RANS models, a popular choice for simulating industrial turbulent flows, are first-order closures. Since all turbulence effects are modeled in such closures, the accuracy of solutions obtained with these models is by definition the lowest from all possible RANS models.

In our research, we are looking for a closure order general enough to be applicable to a wide range of aerodynamic flows, and also able to serve as a foundation for developing lower-order closures in a rigorous manner. Reducing a higher-order closure to a lower-order closure is a physics-based alternative to the existing practice of introducing empirical functions into the transport equations for lower-order turbulence statistics.

In second- and higher-order statistical closures, three processes – turbulent diffusion, dissipation, and interaction of turbulent velocity and pressure fields – have to be modeled. In second-order closures (or Reynolds-stress transport models), terms that describe the turbulent diffusion in the Reynolds-stress transport (RST) equations are usually modeled using the semi-empirical generalized gradient-diffusion hypothesis^{1,5}. This hypothesis is not derived from the analysis of general physical properties of a turbulent flow field. Hence, models based on this hypothesis or of similar kind (see, for example, Chs. 4.3.6 and 4.6 in Refs. 6 and 7) are not physics-based.

The turbulent diffusion modeling can directly be linked to the statistical properties of a turbulent flow field in third-order RANS closures. Millionshtchikov’s hypothesis of quasnormality⁸:

$$\langle u_i u_j u_k u_l \rangle = \langle u_i u_j \rangle \langle u_k u_l \rangle + \langle u_i u_k \rangle \langle u_j u_l \rangle + \langle u_i u_l \rangle \langle u_j u_k \rangle, \quad (1)$$

is based on the assumption of the Gaussian distribution of the probability density function (PDF) of the turbulent velocity field for fourth- and higher-order order velocity moments. When using (1), there is no need for modeling the turbulent diffusion terms in the RST equations; no unknown model coefficient is introduced into the system. In this regard, the accuracy of third-order closures in representing the flow physics has been increased to compare with the accuracy of second-order RANS closures.

The validity of the quasnormality hypothesis was demonstrated for one-point statistics in some experiments starting from [9] and for two-point statistics in [10]. However, a turbulent velocity field is generally non-Gaussian (for detailed discussion, see Ch.6 in Ref. 11). Thus, this closure level should be deemed as insufficient for the most of practical applications.

Fourth-order RANS (FORANS) closures, on the other hand, have all attractive features of third-order closures, but can be closed without assuming Gaussian turbulence. Initial ideas for FORANS closures were considered in Ref. 4. In Ref. 12 various possibilities of representing PDF of a non-Gaussian turbulent velocity field in terms of the degree of its deviation from a Gaussian form were analyzed. The Gram-Charlier series expansions were proposed for this purpose. In such expansions, non-Gaussian PDF is given in the form of a series in Hermite polynomials with respect to the Gaussian distribution. When the Gram-Charlier series expansions are applied to the RANS equations, velocity moments of fifth and higher orders can be represented in terms of lower-order velocity moments in a rigorous manner without any unknown model coefficients¹⁵:

$$\begin{aligned} \langle u_i^5 \rangle &= 10 \langle u_i^2 \rangle \langle u_i^3 \rangle \\ \langle u_i^4 u_j \rangle &= 6 \langle u_i^2 \rangle \langle u_i^2 u_j \rangle + 4 \langle u_i^3 \rangle \langle u_i u_j \rangle \\ \langle u_i^2 u_j^3 \rangle &= 6 \langle u_i u_j \rangle \langle u_i u_j^2 \rangle + \langle u_i^2 \rangle \langle u_j^3 \rangle + 3 \langle u_i^2 u_j \rangle \langle u_j^2 \rangle. \end{aligned} \quad (2)$$

Expressions (2) are derived by truncating the Gram-Charlier series expansions to the fourth order.

The applicability of Gram-Charlier series expansions was successfully tested experimentally in several flows¹³⁻¹⁷. DNS data was used to validate expressions (2) in a 2D channel¹⁸. Currently, DNS data for higher-order statistics in a two-dimensional (2D) zero-pressure gradient (ZPG) boundary layer over a flat plate are also available^{19,20}. Figure 1 shows the comparison of DNS profiles for some of the velocity moments with those obtained from (2) using DNS data for lower-order velocity moments in the ZPG boundary layer. The comparison for the other moments (not shown here) is similar. Although more experimental and DNS data in inhomogeneous flows are desirable, available evidence provides a sufficient basis for choosing Gram-Charlier series expansions to close the set of FORANS equations.

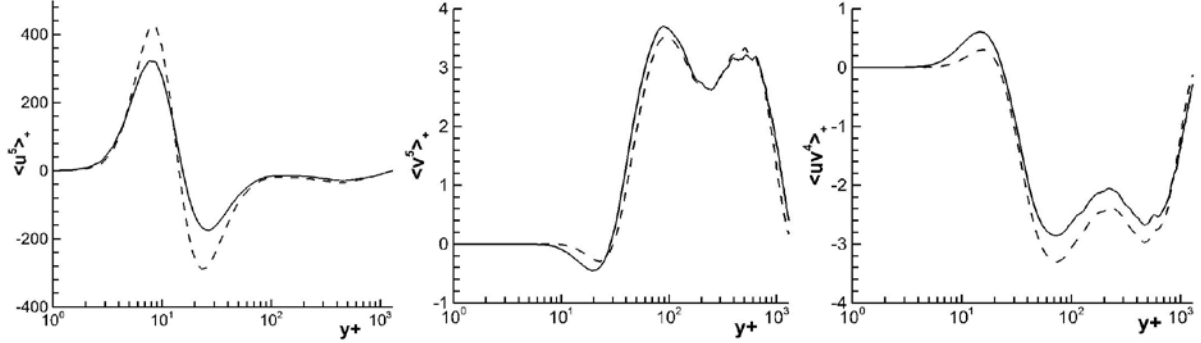


Figure 1. Profiles of fifth-order velocity moments in the ZPG boundary layer over a flat plate ($Re_\theta = 4100$). Notations: — DNS data¹⁸, - - profiles calculated from the Gram-Charlier series expansion representation (2) using DNS data^{18,19} for lower-order velocity moments.

Modeling the dissipation tensor in the RST equations is not a goal of our current research. In transport equations for third- and fourth-order velocity moments, modeling dissipation processes seems to have a negligible effect. This was theoretically predicted in Ref. 4. Later, simulations of the atmospheric boundary layer²¹ and of a fully-developed turbulent flow in an axially rotating cylindrical pipe^{22,23} confirmed this finding. This strategy is currently proposed for the use in FORANS models, but will further be scrutinized in a separate study. The focus of the current paper is on modeling the interaction of turbulent velocity and pressure fields.

II. Modeling the velocity – pressure-gradient correlations

The exact integral-differential expressions for velocity – pressure-gradient correlations of different orders in incompressible flows include “rapid” and “slow” terms along with the surface integrals⁴. In the current study, only modeling the “rapid” and “slow” terms is discussed. The surface integrals can be neglected under the assumption that the length scale of the two - point velocity – pressure correlations is much less than the distance from considered flow points to any flow boundary. Thus, near a wall, the surface integrals should be taken into account and their role there is not negligible²⁴.

For the second-order correlations, the exact expression that includes both “rapid” and “slow” parts takes the following form:

$$-\frac{1}{\rho} \langle p_{,j} u_i \rangle = -\frac{1}{2\pi} \iiint [U'_{m,n} \langle u'_n u_i \rangle'_{,m}]'_{,j} \frac{1}{r} dV' - \frac{1}{4\pi} \iiint \langle u'_m u'_n u_i \rangle'_{,mij} \frac{1}{r} dV'. \quad (3)$$

Expressions for higher-order correlations are similar:

$$-\frac{1}{\rho} \langle p_{,j} u_i u_k \rangle = -\frac{1}{2\pi} \iiint [U'_{m,n} \langle u'_n u_i u_k \rangle'_{,m}]'_{,j} \frac{1}{r} dV' - \frac{1}{4\pi} \iiint [\langle u'_m u'_n u_i u_k \rangle - \langle u'_m u'_n \rangle \langle u_i u_k \rangle]'_{,mij} \frac{1}{r} dV', \quad (4)$$

$$-\frac{1}{\rho} \langle p_{,j} u_i u_k u_l \rangle = -\frac{1}{2\pi} \iiint [U'_{m,n} \langle u'_n u_i u_k u_l \rangle'_{,m}]'_{,j} \frac{1}{r} dV' - \frac{1}{4\pi} \iiint [\langle u'_m u'_n u_i u_k u_l \rangle - \langle u'_m u'_n \rangle \langle u_i u_k u_l \rangle]'_{,mij} \frac{1}{r} dV' \quad (5)$$

Here, Cartesian tensor notations is used; “ ’ ” above a flow variable indicates that it should be evaluated at a point Y' with coordinates x'_i , which ranges over the region of the flow; r is the distance from Y' to the point Y with coordinates x_i ; dV' and dS' are the volume and surface elements, respectively; and $\partial/\partial n'$ denotes the normal derivative. The velocity – pressure-gradient correlations on the left side of (3)-(5) are evaluated at point Y , whereas all derivatives on the right side are taken at Y' .

A. Models for the “rapid” terms

A traditional approach to modeling the “rapid” terms in (3)-(5), that is, integrals with the mean velocity gradients, is based on two fundamental assumptions. One assumption, applicable to all three expressions (3)-(5), is that pressure fluctuations depend on the local mean velocity gradient⁴. This assumption holds true when the function $U'_{m,n}$ varies more slowly than the two-point velocity correlations within the volume determined by the two-point velocity correlation length scale. Then, to a first approximation, the “rapid” term of expression (3) can be re-written as

$$-\frac{1}{\rho} \langle p_{,j} u_i \rangle^{(r)} = -\frac{1}{2\pi} \iiint [U'_{m,n} \langle u'_n u_i \rangle'_{,m}]'_{,j} \frac{1}{r} dV' \approx -\frac{1}{2\pi} U_{m,n} \iiint \langle u'_n u_i \rangle'_{,mj} \frac{1}{r} dV'. \quad (6)$$

“Rapid” terms in (4) and (5) can be simplified in the similar manner. The assumption is expected to be violated close to the wall in boundary layers, which was confirmed in Ref. 24 by analyzing DNS data. It was also shown there that (6) performs well in the logarithmic layer.

The other assumption used in modeling the “rapid” term in (3) is stronger than (6). This is the assumption of turbulence homogeneity²⁵, which imposes an additional condition on the tensor function

$a_{nmji} \approx -\frac{1}{2\pi} \iiint \langle u'_n u_i \rangle'_{,mj} \frac{1}{r} dV'$, such as symmetry under permutation of the indices i and j :

$$a_{nmji} = -\frac{1}{2\pi} \iiint \langle u'_n u_i \rangle'_{,mj} \frac{1}{r} dV' \approx -\frac{1}{2\pi} \iiint \langle u'_{n,m} u_{i,j} \rangle \frac{1}{r} dV'. \quad (7)$$

Various models, linear and non-linear, were proposed for (7) over years including the classical Launder-Reece-Rodi (LRR) model²⁶. However, turbulent flows are usually inhomogeneous. Therefore, to improve the accuracy of simulation results, assumption (7) has to be released. Moreover, this assumption does not help in modeling third- and fourth-order velocity – pressure-gradient correlations.

1. Models based on the local mean velocity gradient assumption.

In this section, modeling expression (6) and similar ones for higher-order velocity – pressure-gradient correlations

$$-\frac{1}{\rho} \langle p_{,j} u_i u_k \rangle^{(r)} = a_{nmjik} U_{m,n} = -\frac{1}{2\pi} U_{m,n} \iiint \langle u'_n u_i u_k \rangle'_{,mj} \frac{1}{r} dV', \quad (8)$$

$$-\frac{1}{\rho} \langle p_{,j} u_i u_k u_l \rangle^{(r)} = a_{nmjikl} U_{m,n} = -\frac{1}{2\pi} U_{m,n} \iiint \langle u'_n u_i u_k u_l \rangle'_{,mj} \frac{1}{r} dV'. \quad (9)$$

are considered.

The properties of a_{nmji} were discussed in Refs. 27, 28 and its model:

$$\begin{aligned}
a_{nmji} &= \frac{1}{5}(\langle u_i u_j \rangle \delta_{mn} + \langle u_i u_m \rangle \delta_{jn}) + \frac{4}{5} \langle u_i u_n \rangle \delta_{jm} + \\
&+ C_1 \left[\frac{1}{2}(\langle u_i u_j \rangle \delta_{mn} + \langle u_i u_m \rangle \delta_{jn}) + k(\delta_{ij} \delta_{mn} + \delta_{im} \delta_{jn}) + \langle u_i u_n \rangle \delta_{jm} - \langle u_j u_m \rangle \delta_{in} - 2(\langle u_j u_n \rangle \delta_{im} + \langle u_m u_n \rangle \delta_{ij}) \right] + \\
&+ C_2 \left[\frac{1}{2}(\langle u_i u_j \rangle \delta_{mn} + \langle u_i u_m \rangle \delta_{jn} - \langle u_j u_n \rangle \delta_{im} - \langle u_m u_n \rangle \delta_{ij}) + k \delta_{in} \delta_{jm} - \frac{3}{2} \langle u_j u_m \rangle \delta_{in} \right]
\end{aligned} \quad (10)$$

was derived there. Expression (10) leads to the following model for the “rapid” part of the velocity – pressure-gradient tensor in the RST equations:

$$\begin{aligned}
\Pi_{ij}^{(r)} &= (a_{nmji} + a_{nmij}) U_{m,n} = -\left(\frac{1}{5} + \frac{1}{2} C_1 + C_2 \right) (\langle u_i u_m \rangle U_{m,j} + \langle u_j u_m \rangle U_{m,i}) + \\
&+ \left(\frac{4}{5} - C_1 - \frac{1}{2} C_2 \right) (\langle u_i u_m \rangle U_{j,m} + \langle u_j u_m \rangle U_{i,m}) + k \cdot (C_1 + C_2) (U_{i,j} + U_{j,i}) - (4C_1 + C_2) \langle u_m u_n \rangle U_{m,n} \delta_{ij}.
\end{aligned} \quad (11)$$

Model (11) transforms to the LRR model²⁶ in homogeneous turbulence²⁸.

The fifth- and six-order tensor functions a_{nmjik} and a_{nmjkl} have properties similar to those of a_{nmji} :

- (i) symmetry under permutation of indices m and j ;
- (ii) if $m = n$, then $a_{mmjik} = a_{mmjkl} = 0$;
- (iii) if $m = j$, then $a_{njjik} = 2 \langle u_n u_i u_k \rangle$ and $a_{njjkl} = 2 \langle u_n u_i u_k u_l \rangle$.

The first property is obvious. The second property follows rigorously from the continuity equation for the two-point velocity correlations⁴: $\langle u'_n u_i u_k \rangle'_{,n} = \langle u'_n u_i u_k u_l \rangle'_{,n} = 0$. The third property results from Green’s theorem under the assumption that the length scale of the two - point velocity correlations is much less than the distance from considered flow points to any flow boundary. Then, the surface integrals can be neglected in Green’s theorem. Close to walls, this assumption may be violated.

Additional property should be imposed on a_{nmjik} and a_{nmjkl} : symmetry in permutation of i and k for the former and of i , k , and l for the latter. Imposing these conditions on the general linear form of the fifth - rank tensor function a_{nmjik} (not shown here) yields the following model expression

$$a_{nmjik} = -\frac{1}{5}(\langle u_i u_j u_k \rangle \delta_{mn} + \langle u_i u_k u_m \rangle \delta_{jn}) + \frac{4}{5} \langle u_i u_k u_n \rangle \delta_{jm}. \quad (12)$$

Then, the model for the “rapid” part of the velocity – pressure-gradient tensor in transport equations for third-order velocity moments is

$$\begin{aligned}
\Pi_{ijk}^{(r)} &= (a_{nmjik} + a_{nmjik} + a_{nmkij}) U_{m,n} = -\frac{1}{5}(\langle u_i u_k u_m \rangle U_{m,j} + \langle u_i u_j u_m \rangle U_{m,k} + \langle u_j u_k u_m \rangle U_{m,i}) + \\
&+ \frac{4}{5}(\langle u_i u_k u_m \rangle U_{j,m} + \langle u_i u_j u_m \rangle U_{k,m} + \langle u_j u_k u_m \rangle U_{i,m}).
\end{aligned} \quad (13)$$

Expression (13) coincides with the expression developed in Ref. 29 by analyzing properties of the pressure - containing correlations in the spectral space in near-homogeneous turbulence.

In the similar manner, the model expression for a_{nmjkl} can be derived (not shown here). The expression includes seven model coefficients. Additionally, it is imposed that

$$\langle u_i u_k u_l p_{,j} \rangle = \langle u_i p_{,j} \rangle \langle u_k u_l \rangle + \langle u_i u_k \rangle \langle p_{,j} u_l \rangle + \langle u_i u_l \rangle \langle p_{,j} u_k \rangle, \quad (14)$$

when turbulence is quasi-Gaussian. In quasi-Gaussian turbulence, equation (1) holds true and transport equations for the fourth-order velocity moments should transform to transport equations for the second-order velocity moments.

The mathematical details are omitted here, but it is easy to show that to satisfy this requirement on the transport equations, expression (14) should be satisfied, in particular. Imposing (14) on the model expression for a_{nmjkl} yields:

$$\begin{aligned}
a_{nmjkl} = & -\frac{1}{5}(\langle u_i u_j u_k u_l \rangle \delta_{mn} + \langle u_i u_k u_l u_m \rangle \delta_{jn}) + \frac{4}{5} \langle u_i u_k u_l u_n \rangle \delta_{jm} + \\
& \left[\frac{1}{2}(\langle u_i u_j \rangle \langle u_k u_l \rangle \delta_{mn} + \langle u_i u_k \rangle \langle u_j u_l \rangle \delta_{mn} + \langle u_i u_l \rangle \langle u_j u_k \rangle \delta_{mn} + \langle u_i u_m \rangle \langle u_k u_l \rangle \delta_{jn} + \langle u_k u_m \rangle \langle u_i u_l \rangle \delta_{jn} + \langle u_i u_m \rangle \langle u_j u_k \rangle \delta_{jn}) + \right. \\
& + C_1 \left[k(\langle u_i u_n \rangle \langle u_k u_l \rangle + \langle u_k u_n \rangle \langle u_i u_l \rangle + \langle u_i u_n \rangle \langle u_j u_k \rangle) \delta_{jm} + \right. \\
& + k(\langle u_k u_l \rangle \delta_{ij} \delta_{mn} + \langle u_k u_l \rangle \delta_{im} \delta_{jn} + \langle u_i u_k \rangle \delta_{jn} \delta_{im} + \langle u_i u_l \rangle \delta_{jn} \delta_{im} + \langle u_i u_l \rangle \delta_{km} \delta_{jn} + \langle u_i u_l \rangle \delta_{jk} \delta_{mn}) - \\
& - \langle u_j u_m \rangle \langle u_k u_l \rangle \delta_{in} - \langle u_j u_m \rangle \langle u_i u_k \rangle \delta_{nl} - \langle u_j u_m \rangle \langle u_i u_l \rangle \delta_{kn} - \\
& \left. - 2(\langle u_j u_n \rangle \langle u_k u_l \rangle \delta_{im} + \langle u_m u_n \rangle \langle u_k u_l \rangle \delta_{ij} + \langle u_m u_n \rangle \langle u_i u_k \rangle \delta_{jl} + \langle u_m u_n \rangle \langle u_i u_l \rangle \delta_{jk} + \langle u_j u_n \rangle \langle u_i u_k \rangle \delta_{im} + \langle u_j u_n \rangle \langle u_i u_l \rangle \delta_{km}) \right] \\
& + C_2 \left[\frac{1}{2}(\langle u_i u_j \rangle \langle u_k u_l \rangle \delta_{mn} + \langle u_i u_k \rangle \langle u_j u_l \rangle \delta_{mn} + \langle u_i u_l \rangle \langle u_j u_k \rangle \delta_{mn} + \langle u_i u_m \rangle \langle u_k u_l \rangle \delta_{jn} + \langle u_k u_m \rangle \langle u_i u_l \rangle \delta_{jn} + \langle u_i u_m \rangle \langle u_j u_k \rangle \delta_{jn}) + \right. \\
& \left. + k(\langle u_i u_k \rangle \delta_{nl} \delta_{jm} + \langle u_i u_l \rangle \delta_{jm} \delta_{kn} + \langle u_k u_l \rangle \delta_{jm} \delta_{in}) - \frac{3}{2}(\langle u_j u_m \rangle \langle u_i u_k \rangle \delta_{nl} + \langle u_j u_m \rangle \langle u_k u_l \rangle \delta_{in} + \langle u_j u_m \rangle \langle u_i u_l \rangle \delta_{kn}) \right] \quad (15)
\end{aligned}$$

where model coefficients are the same as in (10). The model expression for the ‘‘rapid’’ part of the velocity – pressure-gradient tensor in transport equations for fourth-order velocity moments is given as

$$\begin{aligned}
\Pi_{ijkl}^{(r)} = & (a_{nmjkl} + a_{nmjikl} + a_{nmkijl} + a_{nmlijk}) U_{m,n} = -\frac{1}{5}(\langle u_i u_k u_l u_m \rangle U_{m,j} + \langle u_i u_j u_l u_m \rangle U_{m,k} + \langle u_i u_j u_k u_m \rangle U_{m,l} + \langle u_j u_k u_l u_m \rangle U_{m,i}) + \\
& + \frac{4}{5}(\langle u_i u_j u_l u_m \rangle U_{k,m} + \langle u_i u_k u_l u_m \rangle U_{j,m} + \langle u_i u_j u_k u_m \rangle U_{l,m} + \langle u_j u_k u_l u_m \rangle U_{i,m}) + \\
& + (-4C_1 - C_2) U_{m,n} \langle u_m u_n \rangle (\langle u_j u_k \rangle \delta_{il} + \langle u_i u_j \rangle \delta_{kl} + \langle u_i u_k \rangle \delta_{jl} + \langle u_j u_l \rangle \delta_{ik} + \langle u_i u_l \rangle \delta_{jk} + \langle u_k u_l \rangle \delta_{ij}) + \\
& + (-\frac{1}{2}C_1 - C_2) \left(\begin{aligned} & (\langle u_j u_m \rangle \langle u_k u_l \rangle + \langle u_k u_m \rangle \langle u_j u_l \rangle + \langle u_i u_m \rangle \langle u_j u_k \rangle) U_{m,i} + \\ & (\langle u_j u_m \rangle \langle u_i u_k \rangle + \langle u_k u_m \rangle \langle u_i u_j \rangle + \langle u_i u_m \rangle \langle u_j u_k \rangle) U_{m,l} + \\ & (\langle u_i u_m \rangle \langle u_i u_l \rangle + \langle u_i u_m \rangle \langle u_j u_l \rangle + \langle u_i u_m \rangle \langle u_i u_j \rangle) U_{m,k} + \\ & (\langle u_i u_m \rangle \langle u_k u_l \rangle + \langle u_k u_m \rangle \langle u_i u_l \rangle + \langle u_i u_m \rangle \langle u_i u_k \rangle) U_{m,j} \end{aligned} \right) \\
& + (-C_1 - \frac{1}{2}C_2) \left(\begin{aligned} & (\langle u_j u_m \rangle \langle u_k u_l \rangle + \langle u_k u_m \rangle \langle u_j u_l \rangle + \langle u_i u_m \rangle \langle u_j u_k \rangle) U_{i,m} + \\ & (\langle u_j u_m \rangle \langle u_i u_k \rangle + \langle u_i u_m \rangle \langle u_j u_k \rangle + \langle u_k u_m \rangle \langle u_i u_j \rangle) U_{l,m} + \\ & (\langle u_j u_m \rangle \langle u_i u_l \rangle + \langle u_i u_m \rangle \langle u_j u_l \rangle + \langle u_i u_m \rangle \langle u_i u_j \rangle) U_{k,m} + \\ & (\langle u_i u_m \rangle \langle u_k u_l \rangle + \langle u_k u_m \rangle \langle u_i u_l \rangle + \langle u_i u_m \rangle \langle u_i u_k \rangle) U_{j,m} \end{aligned} \right) \\
& + (C_1 + C_2) k \left(\begin{aligned} & \langle u_i u_l \rangle U_{k,j} + \langle u_j u_l \rangle U_{k,i} + \langle u_i u_l \rangle U_{j,k} + \langle u_i u_k \rangle U_{j,l} + \langle u_k u_l \rangle U_{j,i} + \langle u_i u_j \rangle U_{k,l} + \\ & \langle u_i u_k \rangle U_{i,l} + \langle u_j u_l \rangle U_{i,k} + \langle u_k u_l \rangle U_{i,j} + \langle u_i u_j \rangle U_{l,k} + \langle u_i u_k \rangle U_{l,j} + \langle u_j u_k \rangle U_{l,i} \end{aligned} \right). \quad (16)
\end{aligned}$$

The coefficients C_1 and C_2 may vary depending on the flow geometry and the Reynolds number²⁸.

2. Models not based on the local mean-velocity gradient assumption.

As will be discussed in the *Results* section, model expressions (11), (13), and (16) exhibit a deficiency in describing the flow behavior near the wall. Detailed analysis of DNS data and models’ deficiencies led us to conclude that the assumption of the local mean-velocity gradients is at the root of the problem. As a result, new models were derived from considering integrals corresponding to the ‘‘rapid’’ terms in expressions (3)-(5). In the current paper, the initial version of model expressions applicable to 2D planar flows is reported:

$$\begin{aligned}
\Pi_{xx}^{(r)} = & -D_1 (3 \langle v^2 \rangle - 0.5 \langle uv \rangle) U_{,y}, \quad \Pi_{yy}^{(r)} = 1.5 D_1 \langle v^2 \rangle U_{,y}, \\
\Pi_{zz}^{(r)} = & D_1 (1.5 \langle v^2 \rangle - 0.5 \langle uv \rangle) U_{,y}, \quad \Pi_{xy}^{(r)} = 3 D_1 \langle v^2 \rangle U_{,y}. \quad (17)
\end{aligned}$$

$$\begin{aligned}
\Pi_{xxx}^{(r)} = & D_1 (4.5 \langle u^2 v \rangle + 0.5 \langle uv^2 \rangle) U_{,y}, \quad \Pi_{xxy}^{(r)} = D_1 (4.5 \langle uv^2 \rangle - 1.5 \langle u^2 v \rangle) U_{,y}, \\
\Pi_{yyy}^{(r)} = & D_1 (2 \langle v^3 \rangle + \langle uv^2 \rangle) U_{,y}, \quad \Pi_{yyy}^{(r)} = 3.5 D_1 \langle v^3 \rangle U_{,y}, \quad (18)
\end{aligned}$$

$$\begin{aligned}\Pi_{xxxx}^{(r)} &= D_1 (5 \langle u^3 v \rangle - 0.5 \langle u^2 v^2 \rangle) U_{,y}, \quad \Pi_{xxyy}^{(r)} = D_1 (6.5 \langle u^2 v^2 \rangle - 0.5 \langle u^3 v \rangle) U_{,y}, \quad \Pi_{xyxy}^{(r)} = 3D_1 \langle uv^3 \rangle U_{,y}, \\ \Pi_{yyyy}^{(r)} &= D_1 (\langle v^4 \rangle - \langle uv^3 \rangle) U_{,y}, \quad \Pi_{yyyy}^{(r)} = 3.5D_1 \langle v^4 \rangle U_{,y}.\end{aligned}\quad (19)$$

Expressions (17)-(19) were validated in a fully-developed channel flow¹⁸. Expressions (17) were also validated in a ZPG boundary layer over a flat plate using DNS data^{20,30}. Models in the tensor-invariant form will be discussed elsewhere after DNS data for higher-order velocity – pressure-gradient correlations in a ZPG boundary layer is available to validate (18) and (19). Currently, this research is in progress.

B. Models for the “slow” terms

The “slow” terms in (3)-(5) are represented by the following integrals:

$$-\frac{1}{\rho} \langle p_{,j} u_i \rangle^{(s)} = b_{ji} = -\frac{1}{4\pi} \iiint \langle u'_m u'_n u_i \rangle'_{,mnj} \frac{1}{r} dV', \quad (20)$$

$$-\frac{1}{\rho} \langle p_{,j} u_i u_k \rangle^{(s)} = b_{jik} = -\frac{1}{4\pi} \iiint [\langle u'_m u'_n u_i u_k \rangle - \langle u'_m u'_n \rangle \langle u_i u_k \rangle]'_{,mnj} \frac{1}{r} dV', \quad (21)$$

$$-\frac{1}{\rho} \langle p_{,j} u_i u_k u_l \rangle^{(s)} = b_{jikl} = -\frac{1}{4\pi} \iiint [\langle u'_m u'_n u_i u_k u_l \rangle - \langle u'_m u'_n \rangle \langle u_i u_k u_l \rangle]'_{,mnj} \frac{1}{r} dV'. \quad (22)$$

The initial approach to modeling (20) was proposed in Ref. 25. Models for (21) and (22) were suggested in Refs. 17 and 22. However, none of those models is based on the analysis of tensor properties of (20)-(22). The only exception is a model for the “slow” part of the pressure diffusion term in the transport equation for turbulent kinetic energy:

$$-\frac{1}{\rho} \langle u_i p \rangle^{(s)}_i = \frac{1}{5} \langle u_m u_n u_i \rangle_i \quad (23)$$

that was developed in Ref. 29 by analyzing the properties of the pressure - containing correlations in the spectral space in near homogeneous turbulence. For incompressible flows, this model is equivalent to modeling the “slow” part of the velocity – pressure gradient trace. Expression (23) cannot be extended to model integrals (21) and (22) and the “slow” parts of individual components of Π_{ij} .

In the current paper, the tensor functions b_{ji} , b_{jik} , and b_{jikl} are modeled as

$$b_{ji} = B_1 \langle u_m u_{j,m} u_i \rangle, \quad (24)$$

$$b_{jik} = B_1 [\langle u_m u_{j,m} u_i u_k \rangle - \langle u_i u_k \rangle \langle u_m u_{j,m} \rangle], \quad (25)$$

$$b_{jikl} = B_1 [\langle u_m u_{j,m} u_i u_k u_l \rangle - \langle u_i u_k u_l \rangle \langle u_m u_{j,m} \rangle]. \quad (26)$$

Expressions (24)-(26) were derived by analyzing the tensor properties of (20)-(22). They are not the only possible models, but certainly the simplest ones. Due to the length of derivation even for (20), mathematical details are omitted here, but will be reported elsewhere in a different format. Expressions (24)-(26) lead to the following models for the “slow” parts of the velocity – pressure-gradient tensors of second, third, and fourth ranks:

$$\Pi_{ij}^{(s)} = b_{ij} + b_{ji} = -B_1 D_{ij}^{(T)} = B_1 \langle u_m u_i u_{j,m} \rangle, \quad (27)$$

$$\begin{aligned}\Pi_{ijk}^{(s)} &= b_{ijk} + b_{jik} + b_{kij} = -B_1 D_{ijk}^{(T)} = \\ &= B_1 (\langle u_m u_i u_j u_k \rangle_{,m} - \langle u_i u_k \rangle \langle u_m u_{j,m} \rangle - \langle u_j u_k \rangle \langle u_m u_i \rangle_{,m} - \langle u_i u_j \rangle \langle u_m u_k \rangle_{,m}),\end{aligned}\quad (28)$$

$$\begin{aligned}
\Pi_{ijkl}^{(s)} &= b_{jikl} + b_{ijkl} + b_{kijl} + b_{lijk} = -B_1 D_{ijkl}^{(T)} = \\
&= B_1 \left(\langle u_m u_i u_j u_k u_l \rangle_{,m} - \langle u_l u_k u_i \rangle \langle u_m u_j \rangle_{,m} - \langle u_j u_k u_l \rangle \langle u_m u_i \rangle_{,m} - \langle u_l u_j u_i \rangle \langle u_m u_k \rangle_{,m} - \langle u_l u_j u_k \rangle \langle u_m u_l \rangle_{,m} \right),
\end{aligned} \tag{29}$$

where $D_{ij}^{(T)}$, $D_{ijk}^{(T)}$, and $D_{ijkl}^{(T)}$ are the turbulent diffusion tensors in the transport equations for second-, third-, and fourth-order velocity moments. Model expression (27) transforms to (23) in the transport equation for the turbulent kinetic energy.

III. Results

Two sets of model expressions were validated against DNS data^{18,20,30} in 2D planar flows: a fully-developed channel and a ZPG boundary layer over a flat plate. In Set 1, model expressions (11), (13), and (16) for the “rapid” parts of the velocity – pressure-gradient are combined with the corresponding model expressions (27)-(29) for the “slow” parts of the corresponding velocity-pressure tensors. The same model expressions (27)-(29) for the “slow” parts are combined with model expressions (17)-(19) in Set 2.

In Set 1, model coefficients C_1 , C_2 , and B_1 were set to the same values in model expressions for the velocity – pressure-gradient tensors of different orders. In Figure 2, the profiles for Π_{xx} , Π_{yy} , and Π_{xy} obtained using with the DNS data (lines) are compared with the corresponding DNS profiles (solid circles) in a fully-developed channel flow ($Re_\tau = 391.68$). Blue lines correspond to $C_1 = 0.4$, $C_2 = -0.64$, and $B_1 = 0.2$. Red lines are obtained with the same value of B_1 , but $C_1 = 0.3$ and $C_2 = -0.5$. More variations of the coefficients were considered, but the “coefficient tuning” procedure does not eliminate the main deficiency of Set 1, which is a disagreement of model profiles with DNS data at $y_+ < 50$.

A similar tendency is observed for higher-order velocity – pressure-gradient correlations (Figs. 3-4). In Figure 3, model profiles are shown by black lines: solid lines correspond to $B_1 = 0.2$ and dashed lines are obtained at $B_1 = 0.5$. It was found beneficial to vary this coefficient for the correlations of different orders.

In Figure 4, model profiles for fourth-order correlations correspond to two different sets of coefficients. Blue lines are obtained at $C_1 = 0.4$, $C_2 = -0.64$, and $B_1 = 0.8$. Red lines correspond to $C_1 = 0.3$, $C_2 = -0.5$, and $B_1 = 0.8$. In Figures 2-4, all profiles are in viscous units: $\Pi_+ = \Pi \cdot \nu / u_\tau^4$.

Model profiles for second-order correlations were also compared with DNS data in a ZPG boundary layer³⁰ at three Reynolds numbers. Observations were the same as for a channel flow even at higher Reynolds numbers.

To summarize results for Set 1, the near-wall behavior of model profiles deviates from DNS data. This effect is observed in different wall-bounded flows and at different Reynolds numbers. This behavior is due to the assumptions used in deriving model expressions (11), (13), and (16) for the “rapid” terms and should be expected. Outside the buffer zone, Set 1 approximates the main features of the second-, third-, and fourth-order velocity – pressure-gradient correlations profiles. This model will further be tested in free shear flows when DNS data for higher-order correlations are available.

Model profiles obtained with Set 2 are compared with DNS data^{18,20,30} in Figs. 5-9. In Figures 5 and 6, data in a fully-developed channel flow¹⁸ are shown and in Figs. 7-9 in a ZPG boundary layer over a flat plate^{20,30} at $Re_\theta = 300$, 1410, and 4000, respectively. The model coefficient D_1 has the value of 0.3 in all computations. The coefficient B_1 is equal to 0.2, 0.5, and 0.8 in model expressions for second-, third-, and fourth-order correlations, respectively, in different flow geometries and at different Reynolds numbers.

As seen from the figures, Set 2 predicts the behavior of velocity – pressure-gradient correlations in a very close agreement with DNS data everywhere except for very close to the wall, where maximum values of model profiles deviate slightly from the DNS values. In this area, the surface integrals contribution is important^{24,31} and their neglect may be a source of the observed discrepancy. More DNS data for higher-order velocity – pressure-gradient correlations is required to analyze this effect.

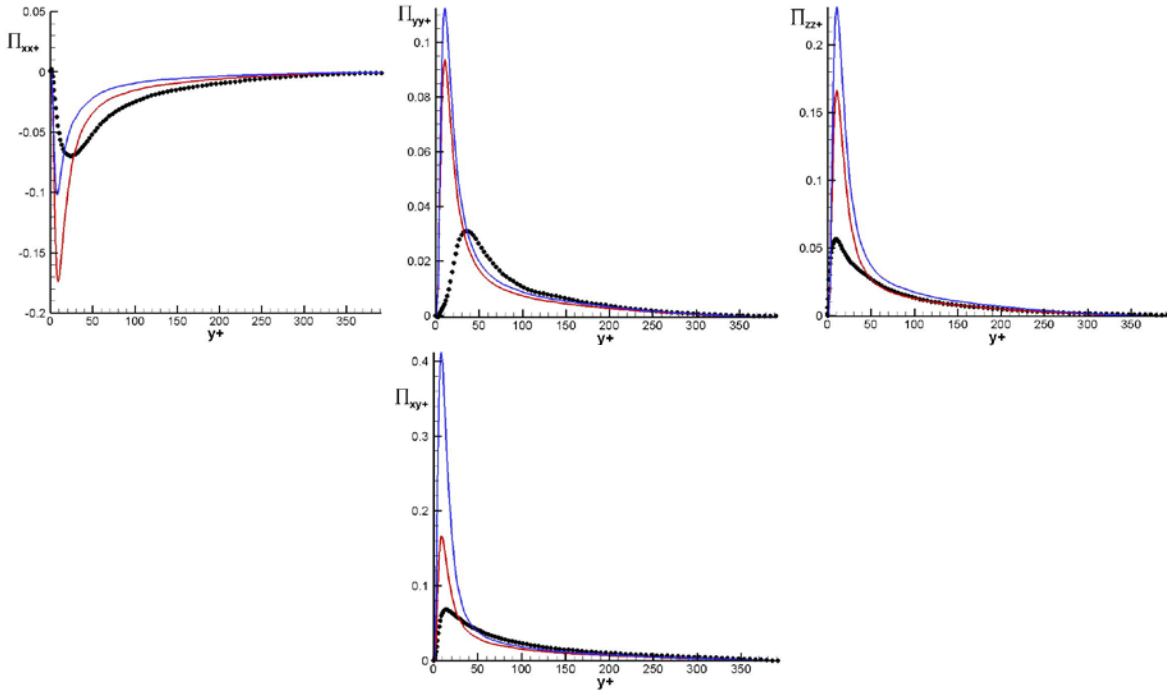


Figure 2. DNS and Set 1 model profiles of second-order velocity – pressure-gradient correlations in a fully developed channel flow ($Re_\tau = 391.68$). Notations: $\bullet\bullet\bullet$ DNS¹⁸; —, —, — Set 1.

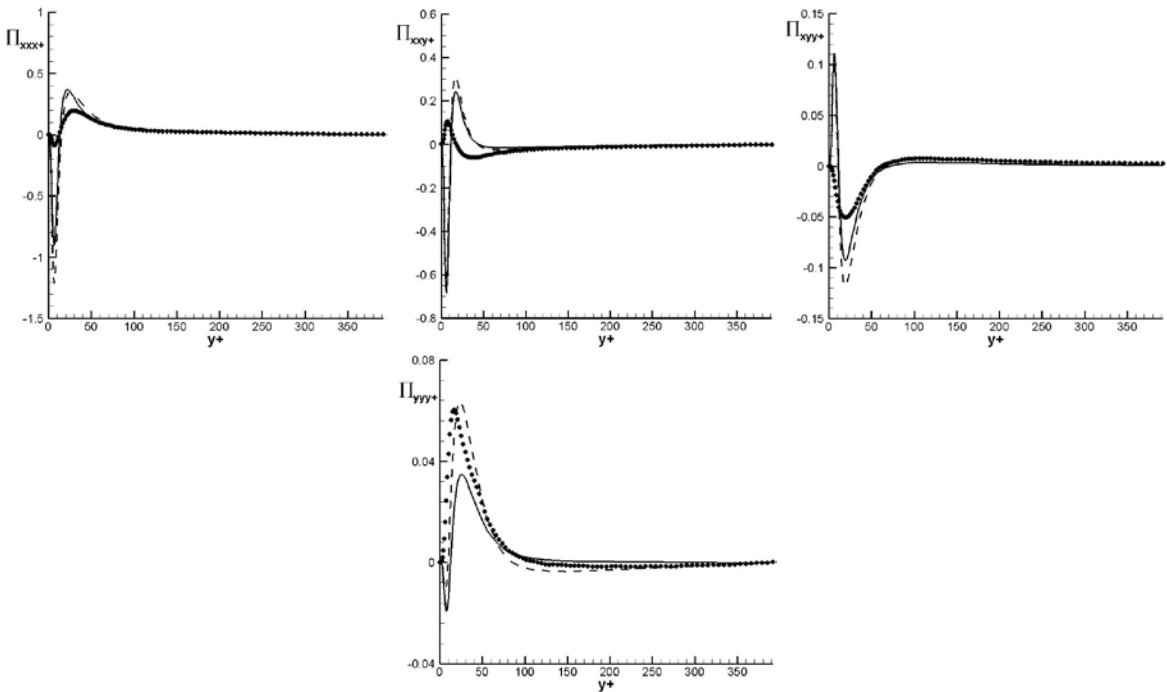


Figure 3. DNS and Set 1 model profiles of third-order velocity – pressure-gradient correlations in a fully developed channel flow ($Re_\tau = 391.68$). Notations: $\bullet\bullet\bullet$ DNS¹⁸; —, - - - Set 1 with $B_1 = 0.2$ and 0.5 .

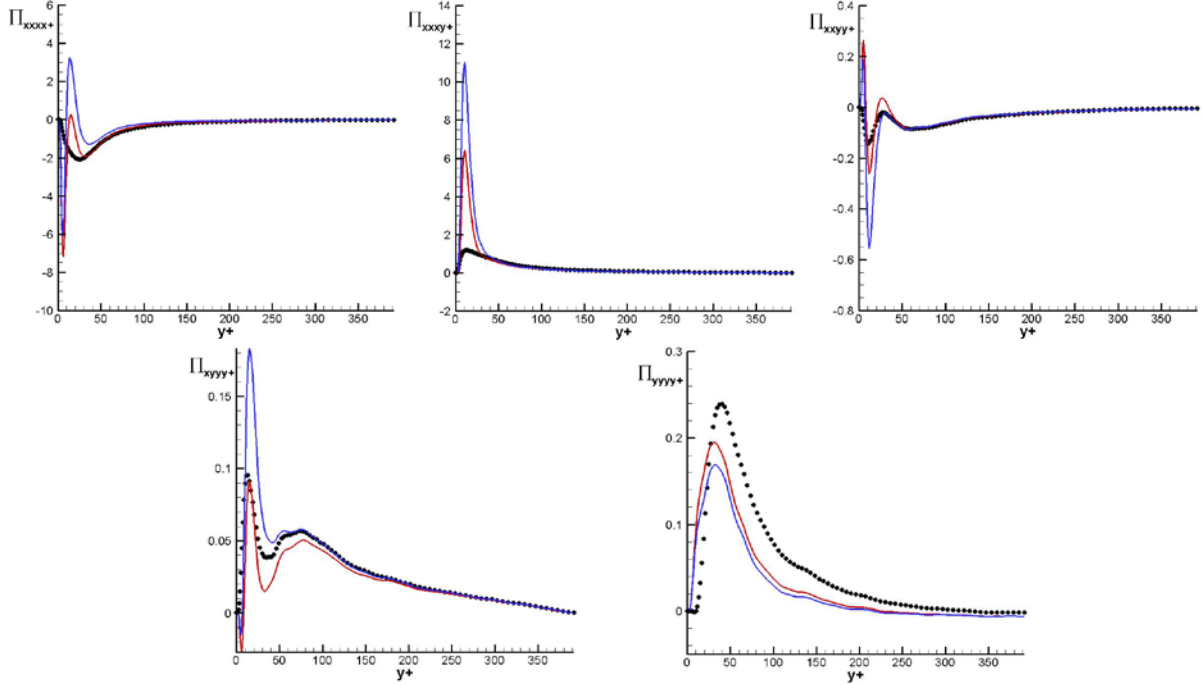


Figure 4. DNS and Set 1 model profiles of fourth-order velocity – pressure-gradient correlations in a fully developed channel flow ($Re_\tau = 391.68$). Notations: ●●● DNS¹⁸; —, —, — Set 1.

IV. Conclusions

In the paper, fourth-order RANS (FORANS) closures are analyzed as a general framework for developing turbulence models applicable to a wide range of aerodynamic flows. Reducing a higher-order closure to a lower-order closure is a physics-based alternative to the existing practice of introducing empirical functions into transport equations for lower-order turbulence statistics to compensate for the lack of physics in such equations.

Of particular interest are FORANS models that utilize the Gram-Charlier series expansions for closing. Such closures are applicable to non-Gaussian turbulent flows and allow for representing fifth- and higher-order velocity moments in terms of lower-order velocity moments in a rigorous manner without unknown model coefficients. Turbulent diffusion terms in transport equations for second- and third-order velocity moments do not require modeling in FORANS models. Recent DNS data for higher-order turbulence statistics in wall-bounded flows such as a flow in a fully-developed channel and a ZPG boundary layer over a flat plate are reviewed in the paper. DNS data confirms previous experimental results that the Gram-Charlier series expansions are applicable in such flows.

The main focus of the paper is on modeling velocity – pressure-gradient correlations in transport equations of FORANS closures. New linear models for the “rapid” and “slow” parts of velocity – pressure-gradient correlations are proposed. A number of model coefficients is fixed, that is, it does not increase with the order of modeled correlations. The “slow” term models include only one coefficient.

Two sets of model expressions for the “rapid” terms were considered. Set 1 is applicable to inhomogeneous turbulent flows where the assumption that the mean velocity gradients vary more slowly than two-point velocity correlations is valid. Set 1 is reduced to the classical Launder-Reece-Rodi model in homogeneous turbulence, where LRR is valid. In this regard, proposed Set 1 is a more general model with a larger potential. In the current study, DNS data were compared with the profiles of second- and higher-order velocity moments obtained with Set 1 combined with the new “slow” term models in a fully-developed channel and in a ZPG boundary layer over a flat plate. The comparison revealed that even this more general model does not well describe near-wall behavior of turbulence statistics. The thorough analysis of data led us to conclude that most likely no model based on the assumption that the mean velocity gradients vary more slowly than two-point velocity correlations will be valid close to a wall. On the other hand, Set 1 is capable to reproduce well DNS data outside the buffer zone.

Set 2 for the “rapid” part of velocity – pressure-gradient correlations was developed to compensate for the near-wall deficiencies of Set 1. It includes only one model coefficient. Very good results were obtained with Set 2

combined with the new “slow” term models without varying the coefficient in different flow geometries and at different Reynolds numbers. Some discrepancy is still observed very close to the wall, but more research and DNS data are necessary to firmly identify sources of this discrepancy.

Acknowledgments

A part of the material is based upon work supported by NASA under award NNX12AJ61A.

References

¹Monin, A. S., Yaglom, A. M., *Statistical Fluid Mechanics: Mechanics of Turbulence. V.1*, 4th printing, MIT Press, Cambridge, Massachusetts, and London, England, 1979, Chap. 4.

²Zagustin, A. L., 1938, “Equations for the turbulent motions of fluids,” *Trudy Voronezh. Univ.*, Vol. 10, No. 2, 1938, pp. 7-39 (in Russian).

³Kolmogorov, A. N., “Equations of turbulent motion of an incompressible fluid,” *Izvestiya AN SSSR, Ser. Fiz.*, Vol. 6, No. 1-2, 1942, pp. 56-58.

⁴Chou, P. Y., “On the velocity correlations and the solutions of the equations of turbulent fluctuation,” *Q. J. Appl. Math.*, Vol. 3, 1945, pp. 38-54.

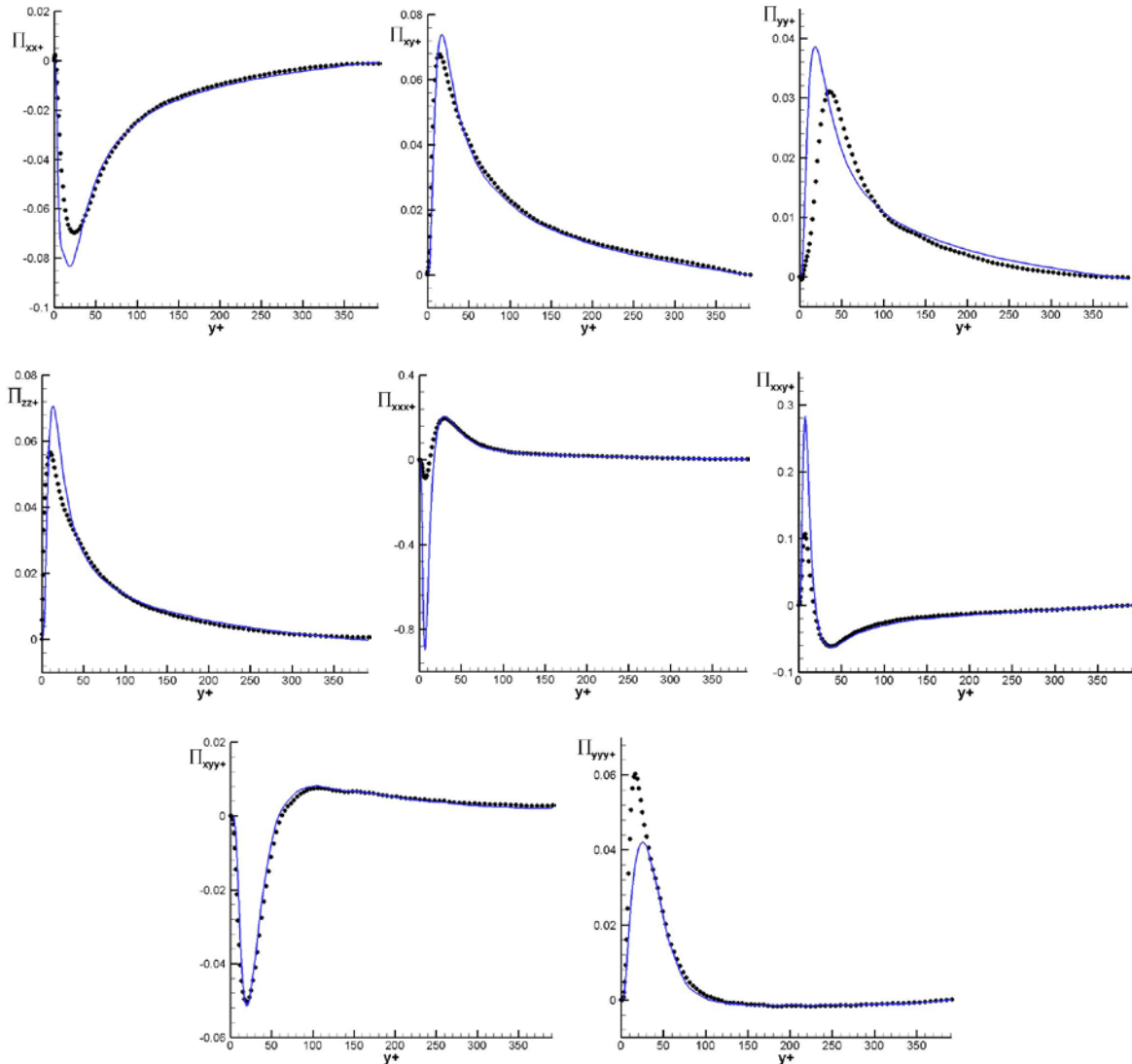


Figure 5. DNS and Set 2 model profiles of second- and third-order velocity – pressure-gradient correlations in a fully developed channel flow. Notations: ●● DNS¹⁸; — Set 2.

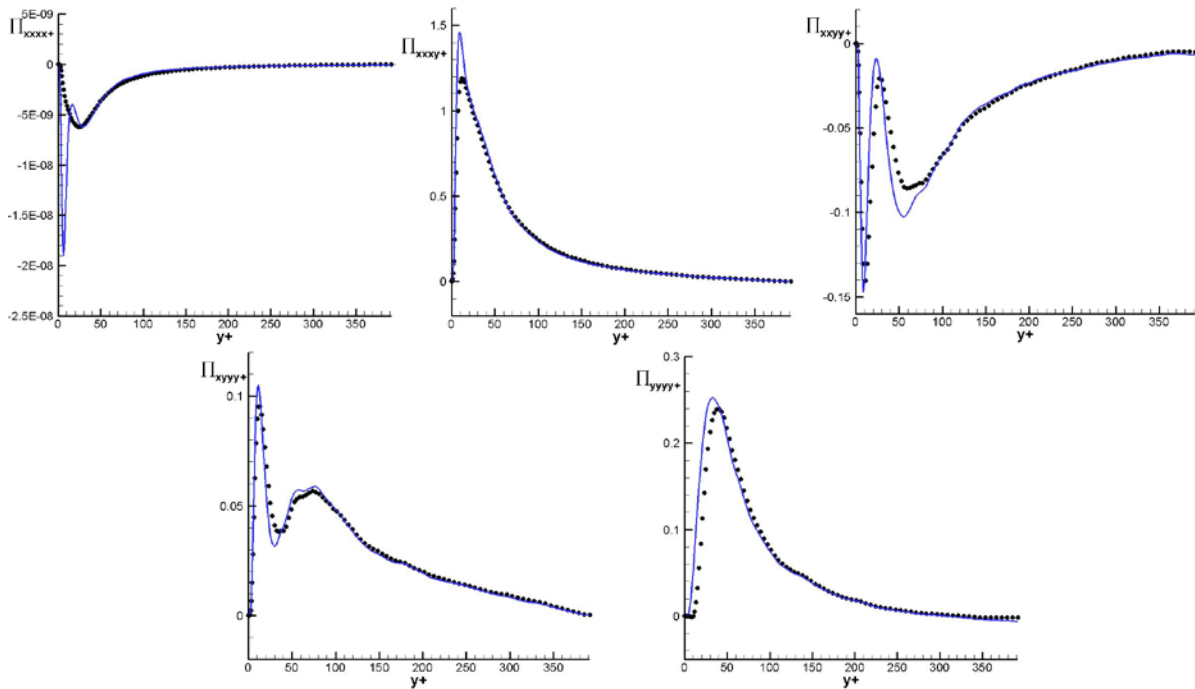


Figure 6. DNS and Set 2 model profiles of fourth-order velocity – pressure-gradient correlations in a fully developed channel flow. Notations as in Fig. 5

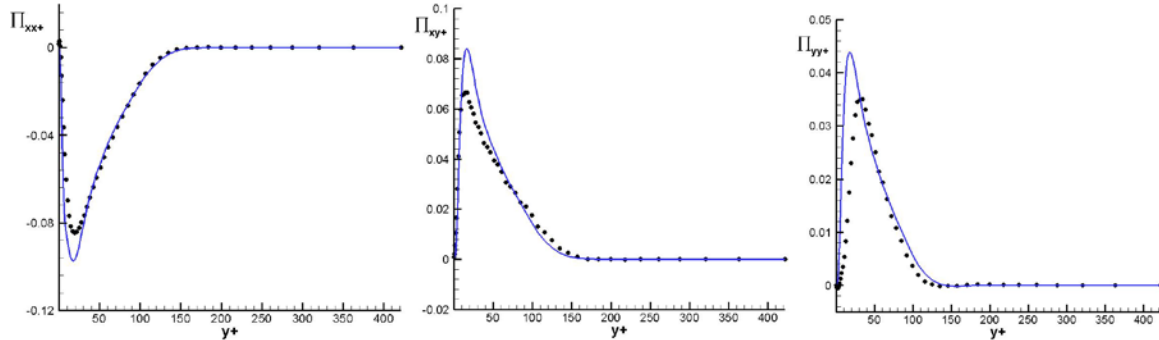


Figure 7. DNS and Set 2 model profiles of second-order velocity – pressure-gradient correlations in a ZPG boundary layer over a flat plate at $Re_\theta = 300$. Notations as in Fig. 5

⁵Daly, B. J., Harlow, F. H., “Transport Equations in Turbulence,” *Phys. Fluids*, Vol. 13, 1970, pp. 2634-2649.

⁶Hanjalić, K., Launder, B., *Modelling Turbulence in Engineering and the Environment*, Cambridge University Press, Cambridge, UK, 2011.

⁷Nagano, Y., Tagawa, M., “Statistical characteristics of wall turbulence with a passive scalar”, *J. Fluid Mech.*, 196, 1988, pp. 157-185.

⁸Millionshtchikov, M. D., “On the theory of homogeneous isotropic turbulence,” *C. R. Acad. Sci. SSSR*, Vol. 32, 1941, pp. 615-619.

⁹Uberoi, M. S., “Quadruple Velocity Correlations and Pressure Fluctuations in Isotropic Turbulence”, *J. Aero. Sci.*, Vol. 20, No.3, 1953, pp. 197-204.

¹⁰Zaets, P. G., Onufriev, A. T., Pilipchuk, M. I., and Safarov, R. A., “Dvukhtocheynye Korrelatsionnye Funktsii Chetvertogo Porydka dlya Prodol’noi Skorosti v Turbulentnom Techenii vo Vrashchayushcheisya Otnositel’no Osi Truby,” (Fourth-Order Two-Point Correlation Functions for the Longitudinal Velocity in a Turbulent Flow in an Axially Rotating Pipe), *VINITI*, Moscow, No. 3831-84, 1984 (in Russian).

¹¹Tsinober, A., *An Informal Introduction to Turbulence*, Kluwer Academic Publishers, 2001, Ch. 6.

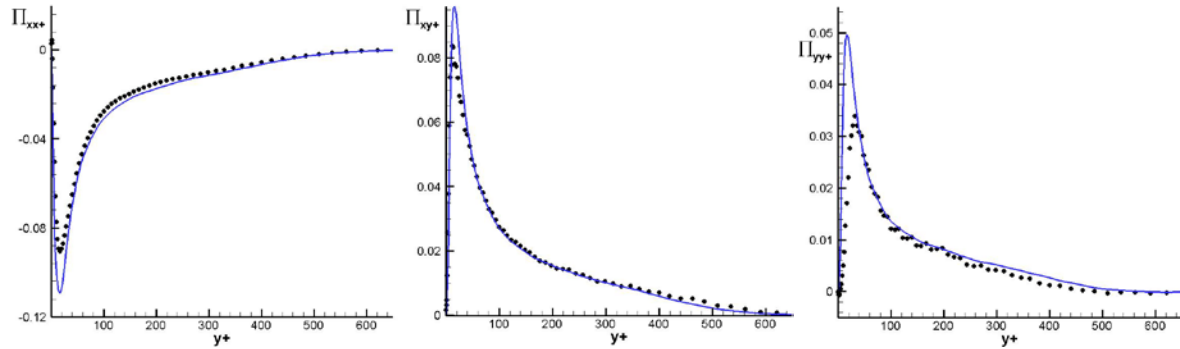


Figure 8. DNS and Set 2 model profiles of second-order velocity – pressure-gradient correlations in a ZPG boundary layer over a flat plate at $Re_\theta = 1410$. Notations as in Fig. 5

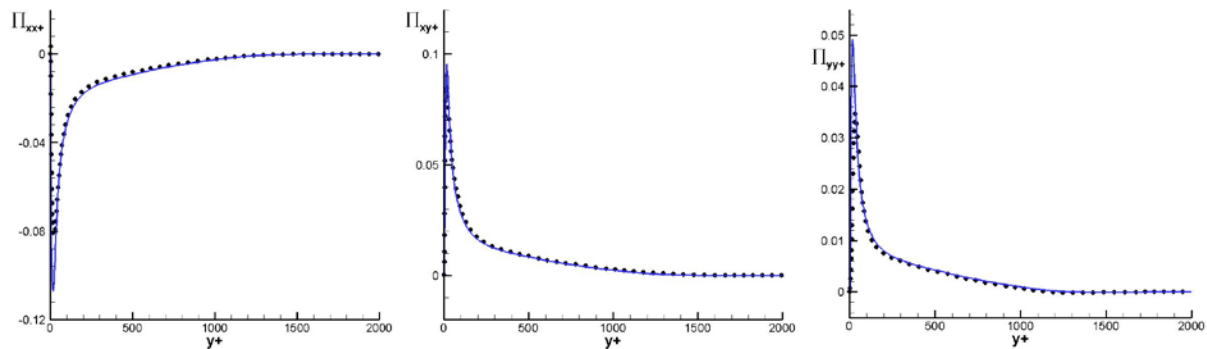


Figure 9. DNS and Set 2 model profiles of second-order velocity – pressure-gradient correlations in a ZPG boundary layer over a flat plate at $Re_\theta = 4000$. Notations as in Fig. 5.

¹²Kampé de Fériet, “The Gram-Charlier Approximation of the Normal Law and the Statistical Description of Homogeneous Turbulent Flow near Statistical Equilibrium,” *David Taylor Model Basin Report No. 2013*, Naval Ship Research and Development Center, Washington D.C., 1966.

¹³Frenkiel, F. N., Klebanoff, P. S., “Probability Distributions and Correlations in a Turbulent Boundary Layer,” *Phys. Fluids*, Vol. 16, No. 6, 1973, pp. 725-737.

¹⁴Antonia, R. A., Atkinson, J. D., “High-order moments of Reynolds shear stress fluctuations in a turbulent boundary layer,” *J. Fluid Mech.*, Vol. 58, No. 3, 1973, pp. 581-593.

¹⁵Durst, F., Jovanović, J., Johansson, T. G., “On the statistical properties of truncated Gram-Charlier series expansions in turbulent wall-bounded flows,” *Phys. Fluids A*, Vol. 4, No. 1, 1992, pp. 118-127.

¹⁶Nakagawa, H., Nezu, I., “Prediction of the contributions to the Reynolds stress from bursting events in open-channel flows,” *J. Fluid Mechanics*, Vol. 80, No. 1, 1977, pp. 99-128.

¹⁷Kurbatskii, A. F., Poroseva, S. V., “A Model for Calculating the Three Components of the Excess for the Turbulent Field of Flow Velocity in a Round Pipe Rotating about its Longitudinal Axis,” *High temperature*, Vol. 35, No. 3, 1997, pp. 432-440.

¹⁸Jeyapaul, E., Coleman, G. N., Rumsey, C. L., “Assessment of Higher-order RANS Closures in Decelerated Planar Wall-bounded Turbulent Flow,” *AIAA Aviation and Aeronautics Forum and Exposition*, Atlanta, GA, June 16-20, 2014.

¹⁹Kaiser, B. E., Sillero, J. A., Poroseva, S. V., “Higher-Order One-Point Statistics for Turbulent Boundary Layer Flow Over a Flat Plate,” 2014 (submitted for review).

²⁰Sillero, J. A., Jiménez, J., Moser, R. D., “One-Point Statistics for Turbulent Wall-Bounded Flows at Reynolds Numbers up to $\delta_+ \approx 2000$,” *Phys. Fluids*, Vol. 25, 105102 (2013); doi: 10.1063/1.4823831, 2013.

²¹André, J. C., De Moor, G., Lacarrère, P., Thierry, G., du Vachat, R., Modeling the 24-hour evolution of the mean and turbulent structures of the planetary boundary layer, *J. Atmos. Sci.*, Vol. 35, 1978, pp. 1861-1883.

²²Kurbatskii, A. F. and Poroseva, S. V. “Modelling turbulent diffusion in a rotating cylindrical pipe flow.” *Int. J. Heat and Fluid Flow*, Vol. 20, No. 3, 1999, pp. 341-348.

²³Poroseva, S. V., *High-order turbulence closure in a fully-developed flow in a cylindrical pipe*, Ph. D. Thesis, Novosibirsk State University, Novosibirsk, 1996 (in Russian).

²⁴Bradshaw, P., Mansour, N. N., and Piomelli, U., “On local approximations of the pressure-strain term in turbulence models,” *1987 Summer Program*, CTR, Report CTR-S87, Stanford University, 1987, pp. 159-164.

²⁵Rotta, J. C., “Statistische theorie nichthomogener turbulenz 1,” *Z.Phys.*, Vol. 129, 1951, pp. 547-572.

²⁶Launder, B. E., Reece, G. J., & Rodi, W., "Progress in the development of a Reynolds-stress turbulence closure." *J. Fluid Mech.*, Vol. 68, No. 3, 1975, pp. 537-566.

²⁷Poroseva, S. V., "New approach to modeling the pressure – containing correlations," *The 3rd Inter. Symposium on Turbulence, Heat and Mass Transfer*. (Nagoya, Japan), 2000, pp. 487-493.

²⁸Poroseva, S. V. "Modeling the "rapid" part of the velocity/pressure-gradient correlation in inhomogeneous turbulence," *Annual Research Brief 2001*, Center for Turbulence Research, NASA-Ames/Stanford University, 2001, pp. 367-374.

²⁹Lumley, J. L. Computational modeling of turbulent flows. *Adv. Appl. Mech.*, Vol. 18, 1978, pp.123-177.

³⁰Spalart, P. R., "Direct simulation of a turbulent boundary layer up to $Re_\theta = 1410$," *J. Fluid Mech.*, Vol. 187, 1988, pp. 61-98.

³¹Skote, M., *Studies of turbulent boundary layer flow through direct numerical simulations*, Ph.D. thesis, TRITA-MEK Tech. Rep. 2001 :01, Dept. Mech., KTH, Stockholm, Sweden, 2001.